Role of Ryanodine Receptors in the Assembly of Calcium Release Units in Skeletal Muscle

Feliciano Protasi,*§ Clara Franzini-Armstrong,* and Paul D. Allen‡§

*Department of Cell and Developmental Biology, University of Pennsylvania, Philadelphia, Pennsylvania 19104-6058;
‡Department of Cardiology, Laboratory of Molecular Cardiology, Children's Hospital, Boston, Massachusetts 02115; and
§Department of Anesthesiology, Brigham and Women's Hospital, Boston, Massachusetts 02115

Abstract. In muscle cells, excitation–contraction (e–c) coupling is mediated by "calcium release units," junctions between the sarcoplasmic reticulum (SR) and exterior membranes. Two proteins, which face each other, are known to functionally interact in those structures: the ryanodine receptors (RyRs), or SR calcium release channels, and the dihydropyridine receptors (DHPRs), or L-type calcium channels of exterior membranes. In skeletal muscle, DHPRs form tetrads, groups of four receptors, and tetrads are organized in arrays that face arrays of feet (or RyRs). Triadin is a protein of the SR located at the SR–exterior membrane junctions, whose role is not known. We have structurally characterized calcium release units in a skeletal muscle cell line (1B5) lacking Ry_1R. Using immunohistochemistry and freeze-fracture electron microscopy, we find that DHPR and triadin are clustered in foci in differentiating 1B5 cells. Thin section electron microscopy reveals numerous SR–exterior membrane junctions lacking foot structures (dyspedic). These results suggest that components other than Ry_1Rs are responsible for targeting DHPRs and triadin to junctional regions. However, DHPRs in 1B5 cells are not grouped into tetrads as in normal skeletal muscle cells suggesting that anchoring to Ry_1Rs is necessary for positioning DHPRs into ordered arrays of tetrads. This hypothesis is confirmed by finding a "restoration of tetrads" in junctional domains of surface membranes after transfection of 1B5 cells with cDNA encoding for Ry_1R.

CALCIUM release units are structures that mediate one step in excitation-contraction (e–c)[1] coupling in muscle cells: the rapid release of calcium from internal stores in response to depolarization of the exterior membranes (Franzini-Armstrong and Jorgensen, 1994; Flucher and Franzini-Armstrong, 1996). Calcium release units are formed by apposed junctional domains of the sarcoplasmic reticulum (SR) on one side, and of exterior membranes (plasma membrane and transverse tubules) on the other. Thin section electron microscopy reveals that the junctional regions of the SR contain foot structures disposed in ordered arrays. The feet, which span the gap between SR and the facing junctional domains of surface membranes (Franzini-Armstrong, 1970), have been identified as the cytoplasmic domains of ryanodine receptors (RyRs) (Kawamoto et al., 1986; Campbell et al., 1987; Imagawa et al., 1987; Inui et al., 1987; Block et al., 1988; Lai et al., 1988; Radermacher et al., 1994). The intramembrane domains of RyRs form the Ca^{2+} release channels of the SR (for reviews see Coronado et al., 1994; Meissner, 1994; Franzini-Armstrong and Protasi, 1997; Sutko and Airey, 1997). During normal muscle contraction, the activation of the SR Ca^{2+} release channels is initiated by a second protein, the dihydropyridine receptor (DHPR), an L-type calcium channel located in exterior membranes (Fosset et al., 1983; Pincon-Raymond et al., 1985; Rios and Brum, 1987; Tanabe et al., 1987, 1988). The direct role of DHPRs in activating muscle contraction was confirmed by lack of e–c coupling (Tanabe et al., 1988) and charge movement (Adams et al., 1990) in dysgenic skeletal muscle, a naturally occurring mouse mutant that fails to express the α_1 subunit of the DHPR (Knudson et al., 1989). In skeletal and cardiac muscles, DHPRs are clustered in junctional domains of exterior membranes facing the arrays of RyRs in the junctional SR (Jorgensen et al., 1989; Flucher et al., 1990, 1994; Yuan et al., 1991; Carl et al., 1995*a*,*b*; Sun

Address all correspondence to Dr. Feliciano Protasi, Department of Anesthesia Research, Brigham and Women's Hospital, 120 Shattuck Street, Boston, MA 02115. Tel.: (617) 278-0597. Fax: (617) 732-6927. E-mail: protasi@zeus.bwh.harvard.edu

1. *Abbreviations used in this paper*: α1-DHPR, α-1 subunit of L-type voltage-dependent Ca^{2+} channel dihidryopyridine receptor; e-c, excitation contraction; ES, embryonic stem; HIHS, heat-inactivated horse serum; RyR, ryanodine receptor; Ry_1R, Ry_2R, and Ry_3R, skeletal isoform of ryanodine receptor, cardiac isoform of ryanodine receptor, and brain isoform of ryanodine receptor; SCID, severly compromised immunodeficient; SR, sarcoplasmic reticulum; T, transverse.

et al., 1995; Protasi et al., 1996). In this position, DHPRs are ideally located to finely control the activation of Ca^{2+} release from RyRs. The mechanism that allows DHPRs to control RyRs activation in skeletal muscle differs from that in cardiac and invertebrate muscles. Skeletal muscle contraction can occur in the absence of external calcium, whereas entry of extracellular calcium through the DHPRs is required for e–c coupling in cardiac and invertebrate muscles (for review see Ashley et al., 1991). The physiologic difference in the e–c coupling mechanism between skeletal and cardiac muscles is reflected in the striking anatomic difference in the arrangements of DHPRs within junctional domains. In skeletal muscle, DHPRs form groups of four, or "tetrads," and tetrads are located in exact correspondence to the four subunits of RyRs (Franzini-Armstrong and Nunzi, 1983; Block et al., 1988; Takekura et al., 1994; Franzini-Armstrong and Kish, 1995; Protasi et al., 1997). This arrangement suggests an e–c coupling mechanism of the type postulated by Schneider and Chandler (1973; for reviews see Schneider, 1981; Rios et al., 1991), in which voltage sensing by the DHPRs results in opening of RyRs by some direct molecular interaction between these two components of the junction. In cardiac muscle, on the other hand, DHPRs are clustered in proximity of RyRs, but they are not grouped into tetrads (Sun et al., 1995; Protasi et al., 1996), and therefore they do not seem to be anchored to RyRs. It is thought that in cardiac muscle Ca^{2+} flux through the DHPRs may act as the activator of the immediately adjacent RyRs, by the "Ca^{2+}-induced Ca^{2+} release mechanism" (Fabiato, 1983; Sham et al., 1995; Santana et al., 1996). This mechanism does not require a DHPR–RyR molecular interaction, but would be facilitated by immediate proximity between the two molecules.

A third molecule located at the junctions between SR and surface membranes, named triadin (Brandt et al., 1990; Kim et al., 1990), has received considerable attention for its possible role in e–c coupling. It is not clear yet whether the molecule is involved in the interaction between RyRs and DHPRs (Caswell et al., 1991; Fan et al., 1995*a*,*b*) or between RyRs and calsequestrin, the calcium-binding protein located in the SR lumen (Knudson et al., 1993*a*,*b*; Guo and Campbell, 1995).

A targeted mutation of the gene encoding the skeletal isoform of the ryanodine receptor (Ry_1R) results in lack of both e–c coupling and feet (hence the term "dyspedic") in skeletal muscles (Takeshima et al., 1994; Takekura et al., 1995*b*; Nakai et al., 1996). We have examined the formation of SR–surface membrane junctions in a dyspedic "muscle" cell line (1B5), derived from a teratoma produced by ES cells with a targeted mutation of Ry_1R (Moore et al., 1998). In these cells, as in the in vivo muscles from a similar targeted mutation (Takekura et al., 1995*b*), junctional SR vesicles dock to the surface membranes in the absence of feet, to form dyspedic junctions. In addition we find that in 1B5 cells triadin and DHPRs do cluster at junctional sites, despite the absence of feet, suggesting that RyRs are not necessary for targeting and clustering those molecules to junctions. However, DHPRs do not form tetrad arrays as in normal skeletal muscle cells, suggesting that some interaction with RyRs must be responsible for the tetradic arrangement of DHPRs. This hypothesis was confirmed by restoration of tetrads after transfection of dyspedic cells with a Ry_1R cDNA. This finding provides direct structural evidence for the requirement of RyR_1 in the formation of DHPR tetrads.

Materials and Methods

The 1B5 Cell Line

The methods used to create the 1B5 cell line are described in detail elsewhere (Moore et al., 1998) but, briefly, it was done in four stages:

Creation of an Embryonic Stem (ES) Cell Line Possessing Two Disrupted ry_1r Alleles. CCS ES cells that had successfully undergone homologous recombination disrupting the ry_1r gene at nucleotide (nt) 840 in exon 10 underwent a second round of selection using high G418 (3.2 μg/ml) to select for the rare homologous recombination of the disrupted allele giving ES cells where both alleles are disrupted (Mortensen et al., 1992).

Creation of Teratomas in Severely Compromised Immunodeficient (SCID) Mice. ES cells that were homozygous for the disrupted ry_1r allele were injected subcutaneously into hind quarters of SCID mice at a concentration of 2–5 × 10^6 ES cells/cm^3 in a volume of 1 cm^3. The injections resulted in ry_1r-/ry_1r- teratocarcinomas composed of several cell types, including 5–10% skeletal muscle. The teratomas were minced, digested with trypsin, and then the cells were plated in growth medium (DME; with 20% FBS, 100 U/ml penicillin, 100 μg/ml streptomycin, and additional 2 mM L-glutamine).

Creation of ry_1r-/ry_1r- Fibroblast Cell Lines. Several primary ry_1r-/ry_1r- fibroblast clonal lines were established.

Creation of Myoblast Cell Line by myoD Infection. Several of the ry_1r-/ry_1r- fibroblast lines were infected with a retrovirus containing a puromycin myoD construct. 48 h after infection, selection was started with puromycin (1 and 2 μg/ml) and clones were picked after 7–10 d. Puromycin-resistant clones were subcloned in growth media. One of the subclones, the 1B5 cell line, was chosen for complete characterization based on its characteristics. It exhibited contact growth inhibition at high density in growth medium and could be induced to differentiate into noncontractile multinucleated myotubes when 5% heat-inactivated horse serum (HIHS) was substituted for 20% FBS in DME medium.

Cell Culturing

The cells were grown at 37°C in growth medium. After 2 d, the cells were replated on thermanox coverslips (Nunc Inc., Naperville, IL) covered with Matrigel (Collaborative Biomedical Products, Bedford, MA). The medium was changed every 2 d. At ~70% confluence, the medium was replaced by a low serum medium (no FBS) containing 5% HIHS to induce differentiation. The differentiation medium was changed every day and the cells were fixed 4–6 d later.

Cell Transfection

The cells were transfected during the growing phase on thermanox coverslips when they reached ~80% confluence. A transfection mixture containing 20 μl of lipofectamine and 3.6 μg of cDNA (in 0.1 ml of Optimem medium) per dish to be transfected was prepared 1 h before transfection and kept at room temperature. Immediately before transfection, 1 ml of Optimem medium was added to the mixture. The growth medium in the dishes was replaced with the transfection mixture and an equal amount of differentiation medium was added 6–8 h later. The transfection mixture was removed 15–20 h later and replaced with differentiation medium. The medium was changed every day and the cells were fixed 4–5 d later.

Immunohistochemistry

Cultures grown on coverslips were fixed either in methanol or acetone for 20 and 10 min, respectively at 20°C, blocked in PBS containing 1% BSA and 10% goat serum for 1 h, and then incubated in primary antibodies overnight at 4°C. After washing four times for 10 min in PBS/BSA, the coverslips were incubated in either FITC-conjugated (Cappel Laboratories, Malvern, PA) or CY3-conjugated (The Jackson Laboratories, Lexington, KY) goat anti–mouse secondary antibodies for 1 h at room temperature, and then washed again. The coverslips were mounted in glycerol containing 0.0025% *para*-phenylenediamine, 0.25% 1,4 diazobicyclo 2,2,2 octane, and 5% *N*-propylgallate to retard photobleaching. The working dilutions and the sources of primary antibodies are listed in Table I. All antibodies

Table I. Antibodies Used for Immunohistochemistry

Specificity (code)	Type	Dilution	Reference
α_1-DHPR (IIF7)	mouse monoclonal	1:100	Leung et al., 1987.
α_1-DHPR (21A6)	mouse monoclonal	1:250	Morton and Froehner, 1987.
α_2-DHPR (20A)	mouse monoclonal	1:250	Morton and Froehner, 1989.
Triadin (GE 4.90)	mouse monoclonal	1:50	Caswell et al., 1991.
RyR 34C	mouse monoclonal	1:2	Airey et al., 1990.

used have been previously characterized. Control slides were not incubated in the primary antibody. The specimens were viewed on a scanning confocal microscope (MRC-600; Biorad Laboratories, Hemel Hempstead, Hertfordshire, England).

Electron Microscopy

The cells were washed twice in PBS at 37°C, fixed in glutaraldehyde, and then kept in fixative for up to 1–4 wk before further use. For thin sectioning, the cells were fixed in 3.5% glutaraldehyde in 0.1 M sodium cacodylate buffer, pH 7.2, followed by 2% OsO_4 for 2 h at room temperature, and then saturated uranyl acetate for 4 h at 60°C. The samples were embedded in Epon 812, and the sections stained in saturated aqueous uranyl acetate followed by lead salts, both for 8 min.

For freeze fractures, the cells were fixed in glutaraldehyde as above, and infiltrated in 30% glycerol. A small piece of the coverslip was mounted with the cells facing a droplet of 30% glycerol, 20% polyvinyl alcohol on a gold holder, and then frozen in liquid nitrogen–cooled propane (Cohen and Pumplin, 1979; Osame et al., 1981). The coverslip was flipped off to produce a fracture that followed the culture surface originally facing the coverslip. The fractured surfaces were shadowed with platinum either at 45° unidirectionally, or at 25° while rotating, and then replicated with carbon in a freeze fracture (model BFA 400; Balzers S.p.A., Milan, Italy). Sections and replicas were photographed in a EM 410 (Philips Electron Optics, Mahwah, NJ).

Measurements

The density of foci in confocal images was measured using the following procedure: (*a*) an area covering 100 μm^2 was selected based on the sharpness of the immunolabeled spots. This selection procedure accepts areas in which the optical section grazes the surface membrane and excludes areas where the focal plane is below the cell surface and the spots are diffuse; (*b*) the contrast was increased to bring the spots to saturation. Under these conditions the large majority of spots are very well defined (see detail in Fig. 7 *B*); (*c*) the spots were counted; and (*d*) two or three measurements were performed in different areas for each cell. For more details about foci counting see Fig. 7 legend.

The width of the junctional gap between SR and surface membranes was measured along lines drawn at several random positions across the junctions, using a dissecting microscope fitted with an eyepiece micrometer.

The density of large membrane particles was calculated from counts of all junctional domains and several randomly selected nonjunctional domains in micrographs with excellent shadow quality (comparable to the one shown in Fig. 6).

The apparent diameter of intramembranous particles was measured at right angle to the direction of platinum deposition. The thickness of platinum deposition is closely monitored using a quartz thin film monitor; thus variations in apparent particle diameter because of this factor are small. The approximate particle height was determined by measuring the length of the platinum-free "shadow." The length of the shadow is influenced by the angle of platinum shadowing and this in turn is affected by curvature of the shadowed membrane. Variations resulting because of shadowing angle are minimized by avoiding micrographs with obviously foreshortened or elongated shadows. Particles clustered within junctional domains and visually identified as large were measured until a count of 100 was reached. All particles within regions of approximately equal size, but showing no sign of large-particle clustering, were measured until the same total count was reached.

The density of large particle clusters on the surface membrane was calculated from counts of electron micrographs at magnifications between 20,000 and 44,500. The density of immunoreactive spots was calculated from counts of digitized images enlarged ~10,000 fold.

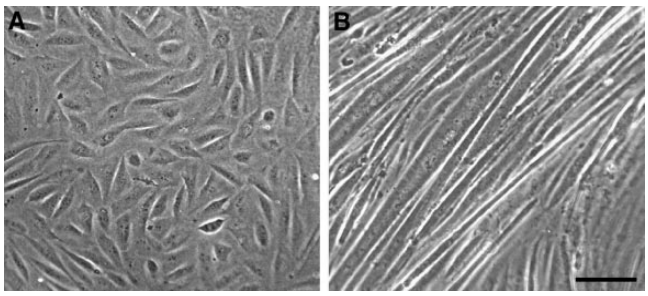

Figure 1. (*A*) Undifferentiated 1B5 cells in presence of growth medium are small, mostly fusiform, and mononucleated. (*B*) 6 d after withdrawal of growth medium differentiated myotubes are quite large and usually in a monolayer. Bar, 100 μm.

Results

Dyspedic Calcium Release Units in 1B5 Cells

1B5 cells cultured in presence of growth factors are usually small, fusiform, and mononucleated (Fig. 1 *A*). After withdrawal of growth factors, most cells fuse and differentiate into aligned multinucleated myotubes, some 50 μm or more in width (Fig. 1 *B*).

Immunohistochemistry. Differentiated 1B5 cells were immunolabeled with antibodies specific for junctional proteins of exterior membranes (α_1 and α_2 subunit of the DHPR) and SR (triadin). 5 d after withdrawal of growth medium, about a third of the myotubes are positive for these antibodies. α_1- and α_2-DHPR and triadin are clustered in discrete foci, similar to those found in normal skeletal developing muscle and in adult skeletal and cardiac muscle (Figs. 2 and 3; compare with Yuan et al., 1991; Flucher et al., 1993*b*, 1994; Knudson et al., 1993*a*; Guo et al., 1994, 1996; Carl et al., 1995*a*,*b*). The majority of immunopositive spots are located on or near the surface membrane, on both ventral and dorsal sides of the myotubes (Fig. 2; see Fig. 3 for a through focus series). The images cannot distinguish between foci of immunofluorescence at the surface of the cell and in the cortical cytoplasm (Yuan et al., 1991). The ventral side of the cell, facing the coverslip, is flat and thus gives the best images (Fig. 2).

Since the two antibodies used for the immunochemistry are both derived from mouse, we did not attempt double immunolabeling. However, several observations indicate that the location of DHPR- and triadin-positive foci coincide. First, the density of triadin-positive foci at or close to the coverslip-facing side of the cell (35.8 ± 9.6/100 μm^2 from 65 measurements in 25 cells, 23 confocal images, mean ± 1 SD) is very similar to the density of DHPR foci (38.8 ± 7.0/100 μm^2 from 102 measurements in 33 cells, 34 confocal images). Second, when the cells were colabeled with both antibodies (anti–α_1-DHPR and anti-triadin) the density of foci at or close to the coverslip-facing side of the

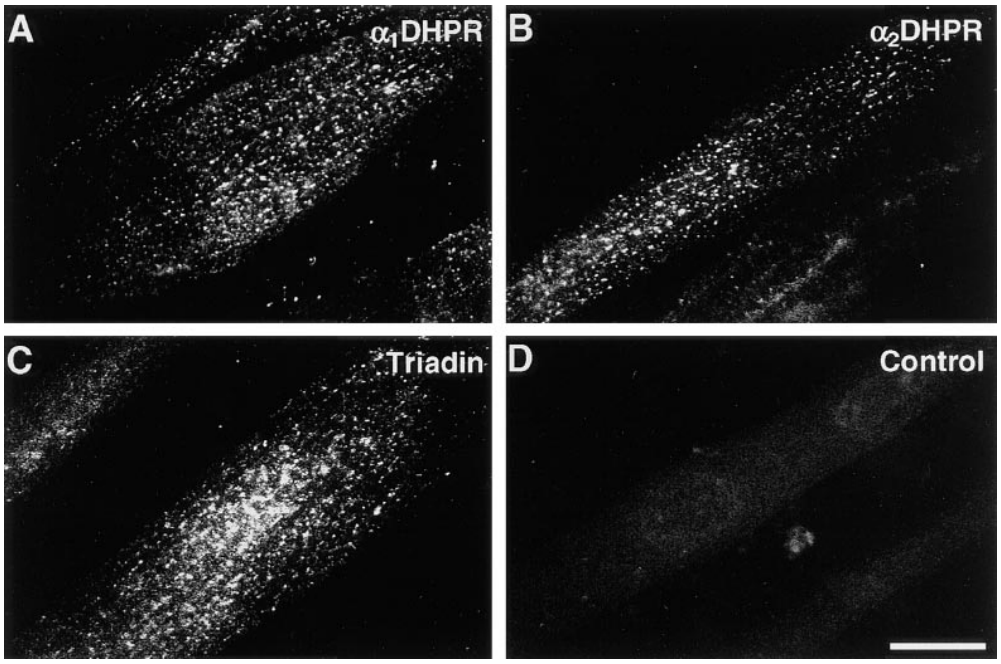

Figure 2. Immunofluorescence labeling of 1B5 cells 5 d after differentiation, with antibodies against α_1-DHPR (*A*), α_2-DHPR (*B*), and triadin (*C*). No primary antibodies were used in the control image (*D*). The plane of focus is close to the substrate side of the cell, which is flat. The two DHPR subunits and triadin cluster in frequent, discrete foci at or near the cell surface (see Fig. 3). About a third of the cells in differentiated cultures react with any of the three antibodies in the manner shown here. The densities of DHPR and triadin foci are approximately equal (see text). Bar, 25 μm.

cells is practically identical to that obtained by single labeling with either antibody (36.3 ± 5.5/100 μm^2 from 52 measurements in 17 cells, 16 confocal images). If the two molecules were not colocalized we would definitely expect a higher number of positive foci (approximately double). In addition, the intensity of foci was definitely higher in the case of cells stained with both antibodies than in cells stained in parallel with either antibody alone. A third observation indicating coincidence of DHPR and triadin foci is that they are similarly disposed over the cell surface (see Figs. 7 and 8; and see below).

Electron Microscopy, Thin Sections. Differentiating 1B5 cells develop somewhat disordered and defective myofibrils containing variable amounts of myofibril components. More differentiated cells have A bands that tend to be randomly oriented and spaced, and with aligned thick filaments and a clear M line (Fig. 4 *A*, *arrows*). There is no evidence of Z lines, and a smaller than normal complement of thin filaments is present (Fig. 4 *B*).

Primitive transverse (T) tubules (or plasma membrane invaginations) and SR systems are present in all differentiating cells containing developing myofibrils, and are absent in cells that do not show any evidence of myofibrillogenesis. T tubule–like invaginations are located at the fiber periphery, mostly within a subcortical strip of cytoskeleton devoid of myofibrils. These invaginations appear most frequently as apparently empty, wide vesicles with a well-demarcated membrane (Fig. 5, *C–E*), and less frequently as labyrinthine networks resembling multiple caveolae (Fig. 4 *C*, *arrows*) (Ishikawa, 1968; Franzini-Armstrong, 1991). The continuity between these vesicles and the fiber surface can be directly traced in some instances (data not shown). There is no evidence of a mature T tubule network penetrating between the myofibrils and associating

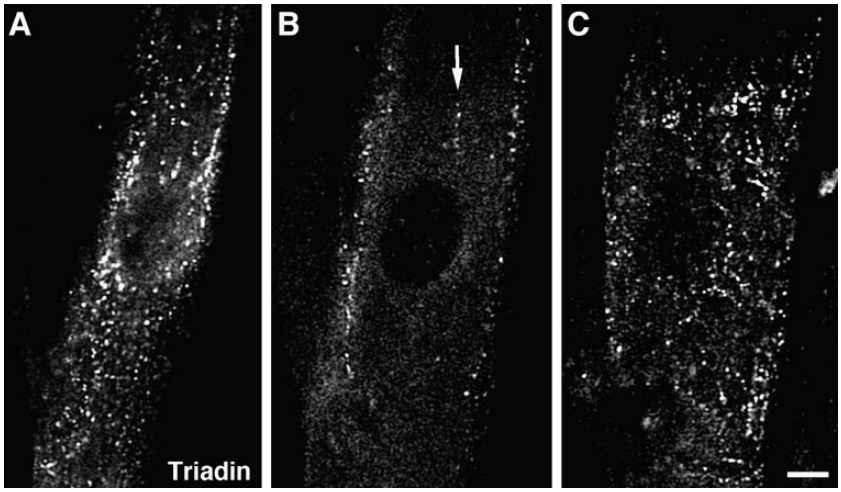

Figure 3. Triadin immunolocalization in a 1B5 cell at 5 d after differentiation. Through focus images at the top (*A*), middle (*B*), and bottom (*C*) of the cell show that the triadin foci are predominantly located on, or in proximity of, the plasma membrane. When the optical section bisects the cell, foci are at the cell edge, and few are located in the fiber interior (*B*, *arrow*). Identical results were obtained using antibodies against DHPR subunits. Bar, 10 μm.

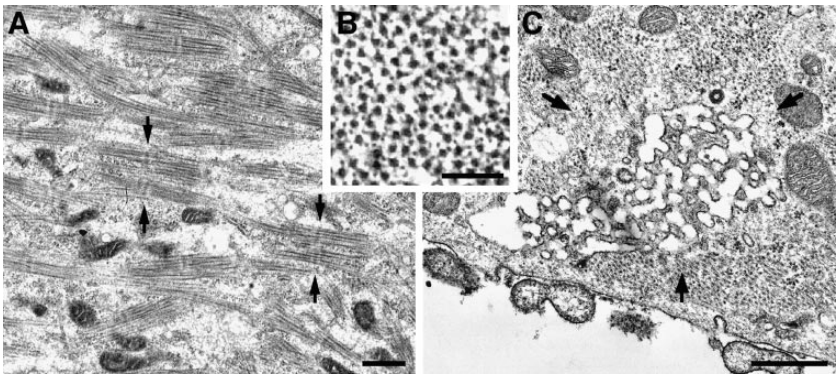

Figure 4. (*A*) The cytoplasm of differentiated 1B5 cells 5 d after differentiation contains bundles of thick filaments arranged in complete A bands with evident M lines (*between arrows*), but Z lines are either missing or incomplete. (*B*) Incomplete sets of thin filaments overlap with the thick filaments in this cross section of a myofibril. (*C*) A labyrinthine membrane network (*arrows*) is an initial step in the development of a T tubule system. Such networks are rarely seen. Other primitive T tubules appear as short, wide invaginations (see Fig. 5). Bars: (*A* and *C*) 0.5 μm; (*B*) 0.1 μm.

with them. Few primitive T tubules (identifiable by their proximity to an SR element, see below) are present in the fiber interior in proximity of the Golgi regions.

Numerous small vesicles with an electron dense content are closely apposed either to the plasma membrane (Fig. 5, *A–C*), or to short T tubules (Fig. 5, *C–E*). The junctions thus formed closely resemble peripheral couplings and dyads (Fig. 5 *F*) of normal developing myotubes. We identify the vesicles as SR elements and their electron-dense content presumably represents calsequestrin (Meissner, 1975). Nonjunctional or free SR is scarce. All visible T tubule profiles have at least one SR vesicle associated with them, and thus the densities of junctions along the plasmalemma and in the subcortical and deeper regions of the cell depend on the extent of T tubule development. The free surface of the cells has numerous, short, developing T tubules. On the free side of the cell, 39% of the junctions are peripheral couplings, and 61% are peripherally located dyads (from a total of 193 junctions, from 26 cells). On the other hand, on the substrate side, T tubules are less numerous and peripheral couplings account for 64% of the junctions, whereas peripherally located dyads are only 36% of the total (from 152 junctions, 25 cells). Junctions within the cell interior are rare (43, or 11%, out of a total of 388 junctions in all locations), and they are usually in small clusters within some, but not all, cell profiles. The lo-

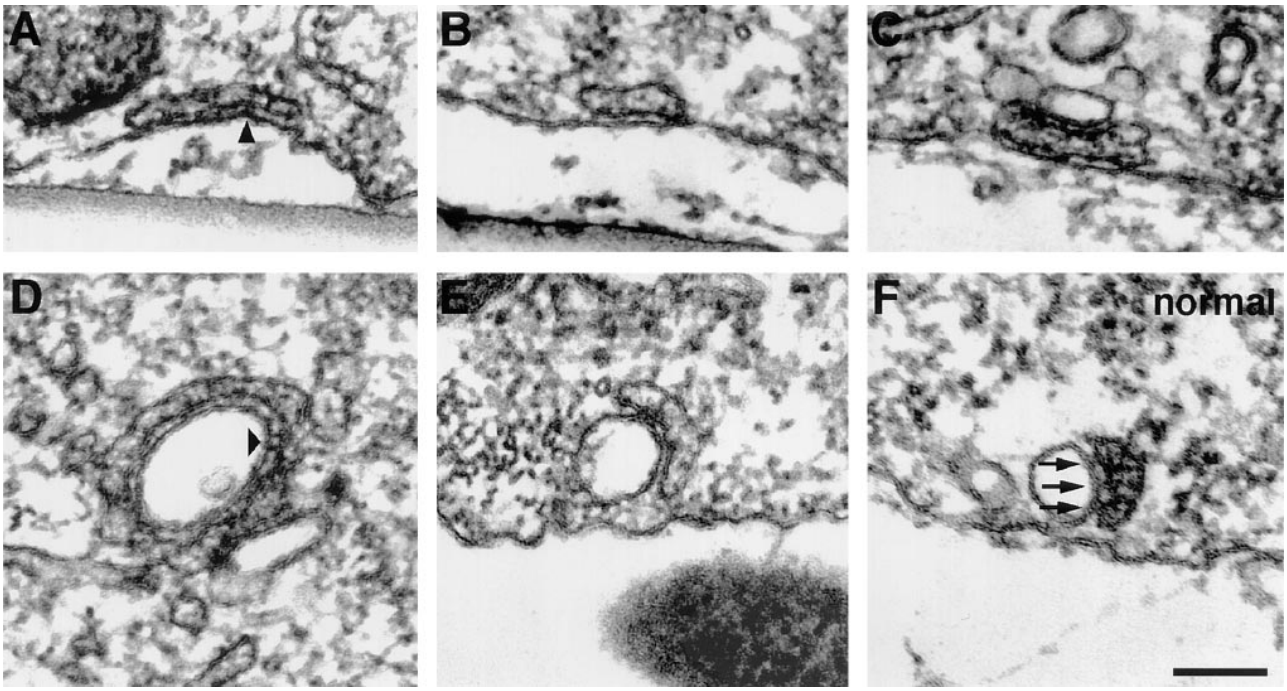

Figure 5. Dyspedic junctions in 1B5 cells at 5 d after differentiation (*A–E*), compared to a normal junction from in vivo mouse diaphragm (*F*). Junctions between SR and the plasma membrane (peripheral couplings; *A* and *B*), and junctions between SR and primitive T tubules (dyads; *E*) are present. The SR profile in *C* makes contact with the plasma membrane on one side, and a T tubule on the other. The SR profiles have a dense content, whereas the surface invaginations have an empty lumen. In dyspedic junctions (*A–E*), the junctional gap is too narrow to accommodate feet, so the small densities visible in the junction (*A* and *D*, *arrowheads*) are due to proteins other than RyRs. Note larger gap occupied by evenly spaced feet (*F*, *arrows*) in the normal junction. Bar, 0.1 μm.

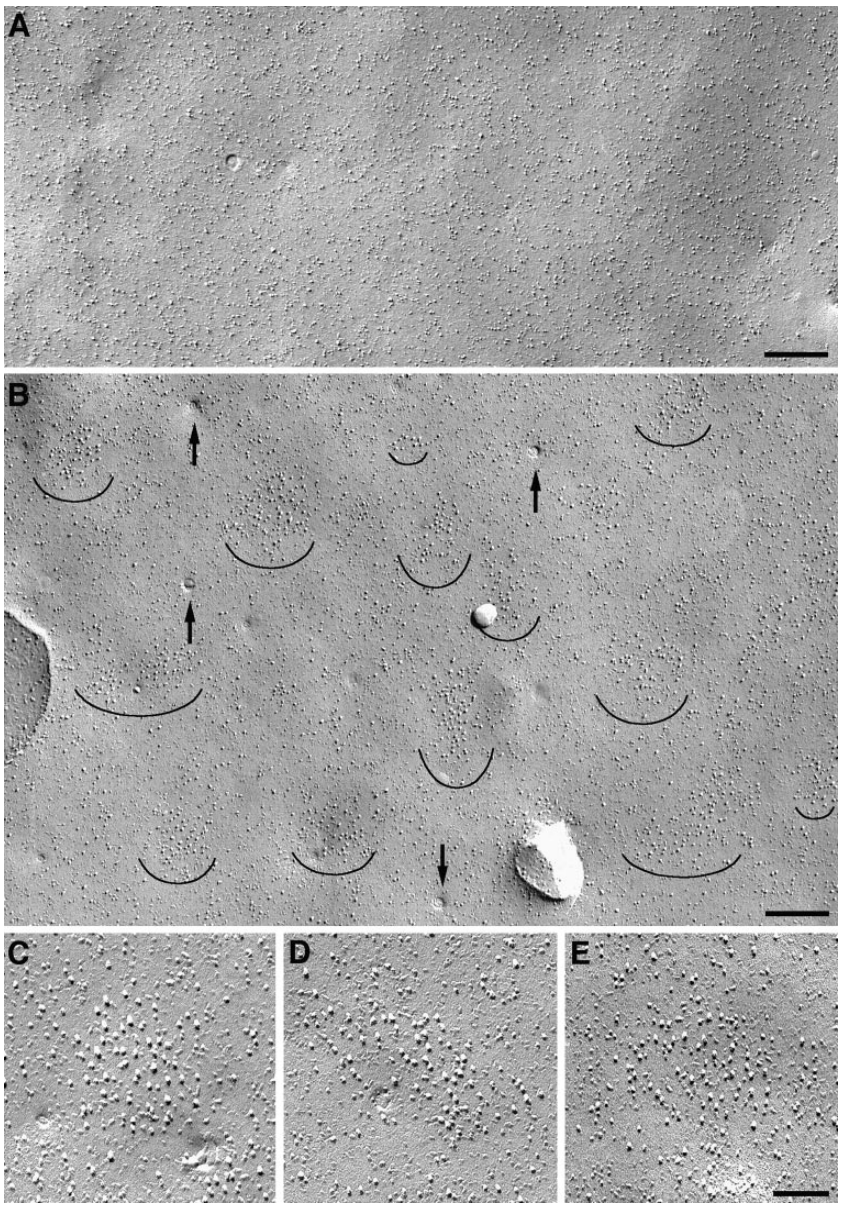

Figure 6. Internal leaflet of the plasma membrane in freeze-fracture replicas of undifferentiated and differentiated cells. (*A*) The membrane of undifferentiated cells in the presence of growth factor is characterized by intramembrane particles that are randomly distributed and that do not form any particular grouping. (*B*) After withdrawal of growth factors 5 d after differentiation ~35% of the cells contain clusters of intramembrane particles (plasma membrane domains; *semicircles*) that are taller and larger than the average. (*C–E*) Details of plasma membrane domains, 5–6 d after differentiation no order is detectable in the distribution of large particles within these domains. Bars: (*A* and *B*) 0.2 μm; (*C–E*) 0.1 μm.

cation of the junctional SR vesicles at or close to the fiber periphery agrees well with the location of the DHPRs and triadin foci seen by immunohistochemistry, which are at or near the surface of the cell (Fig. 3).

All junctions in 1B5 cells are dyspedic, i.e., "feet" are absent from the junctional gap between SR and exterior membranes, and the gap width is narrow (Fig. 5, *A–E*). On the average, the junctional gap is 6.5 ± 2.6 nm (mean ± 1 SD, $n = 52$ junctions, 37 peripheral couplings and 15 dyads, 255 measurements) and thus too small to accommodate cytoplasmic domains of RyRs or feet, which are ~12-nm wide (Radermacher et al., 1994). The irregularly disposed strands that usually occupy the gap in dyspedic myotubes (Fig. 5, *A* and *D*, *arrowheads*) are clearly composed of a protein different from RyR. The gap in feet-containing junctions from normal myotubes is wider (Fig. 5 *F*, from a normal in vivo myotube). Gap widths of 10–13 nm have been previously measured in junctions from mouse myotubes developing in vivo (Takekura et al., 1995*b*) and in vitro (Nakai et al., 1997) fixed and stained as in this study. Junctions with a 10–13-nm gap were not detected in 1B5 cells.

Electron Microscopy, Freeze Fracture. In freeze fracture replicas of undifferentiated cultures the cytoplasmic leaflet of the plasmalemma is smooth and it shows intramembrane particles of variable sizes, without any sign of clustering (Fig. 6 *A*).

The plasma membranes of large myotubes in differentiated cultures have dimples marking the mouths of caveolae and T tubules (Fig. 6 *B*, *arrows*) and plasma membrane domains that contain clusters of large, tall particles (Fig. 6 *B*, *semicircles*). Small- and medium-sized particles are largely excluded from these clusters (see details in Fig. 6, *C–E*). The apparent diameter and height of large particles in plasma membrane domains is 9.9 ± 1.7 nm and 10.9 ± 1.5 nm, respectively (mean ± 1 SD; $n = 100$, 4 cells, 4 freeze fractures). The apparent diameter and height of particles, including large ones, in patches of membrane adjacent to

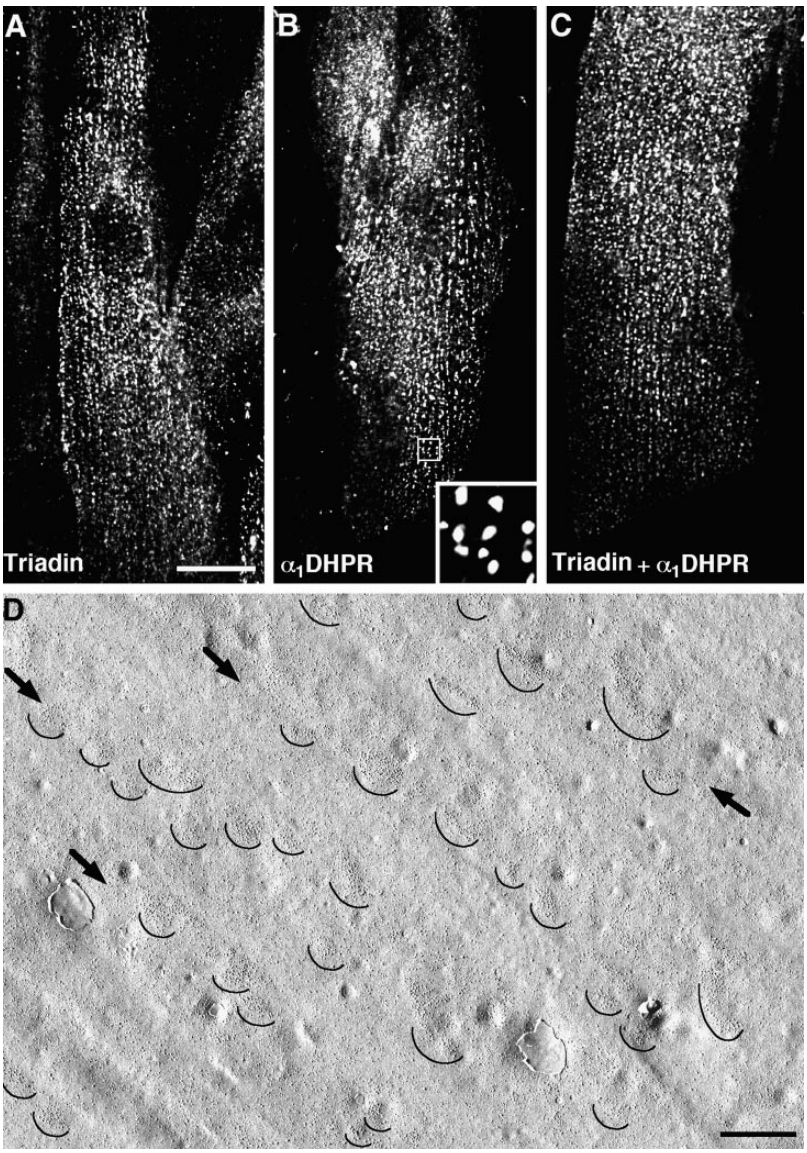

Figure 7. Analogies in the distribution of triadin and DHPR foci, and of particles clusters. (*A–C*) Cells immunolabeled respectively with anti-triadin, anti–α_1-DHPR, and both antibodies. The density of clusters in all three samples is very similar (see Results) suggesting a colocalization of the two structures. Note also the tendency for an alignment of the clusters into longitudinal lines, along the long axis of the cell. The foci density was measured using the procedure detailed in the Materials and Methods section. An area prepared for counting by enlarging five times and increasing the contrast is shown as a detail in *B*. The 25-μm^2 area contains 12 foci. Counting was done in portions of the images where the focal plane grazes the cell surface (e.g., Figs. 7, *A* and *C*, middle areas), whereas areas in which the optical section either includes the underlying cytoplasm, or moves too far from the cell surface (e.g., Fig. 7, *B*, *top/left* region; and *C*, *bottom*) were avoided. (*D*) Freeze-fracture. The locations of particles clusters in the plasma membrane are marked by semicircles. The frequency of particles clusters is similar to the density of foci positive for triadin and α_1-DHPR and they are similarly aligned in longitudinal rows in some cells (*arrows*). The long axis of the cell is aligned vertically in *A–C* and diagonally in *D*, as is the orientation of foci and particle cluster lines. Bars: (*A–C*) 20 μm; (*B*) 0.5 μm.

the cluster-containing domains is 6.8 ± 1.5 nm (n = 100) and 6.5 ± 1.8 nm (n = 100), respectively. Differences between diameters and heights in the two groups are extremely significant (Student's t test; $P < 0.0001$ in both cases). Note that the large-clustered particles are also relatively tall; their height to diameter ratio is 1:10, whereas the ratio in random particles is 0.95. The average density of large particles in junctional plasma membrane domains is 1,077 ± 228/μm^2 (n = 63; mean ± 1 SD; n = number of domains), whereas the average density of large particles in nonjunctional regions is 104 ± 57/μm^2 (n = 82). The differences between the two data are large and extremely significant (Student's t test $P < 0.0001$) confirming the visual observation of clustering.

In D5–6 cultures 35% of the cells (from a total of 334 cells in 7 cultures, 11 replicas) contain plasma membrane domains with clusters of large particles (Fig. 6, *B–E*). The surface of the rest of the cells resemble that of cells fixed in the presence of growth medium (Fig. 6 *A*). We could not determine whether the presence of particle clusters is limited to multinucleated cells.

Identification of Clusters of Particles with DHPR Foci and Clues to Their Junctional Location. Foci of DHPRs detected by immunolabeling and clusters of large intramembrane particles are present at comparable densities. The two densities, related to the apparent surface area, are 38.8 ± 7.0/100 μm^2 (from 102 measurements in 33 cells, 34 confocal images, detected by the α_1 antibody) and 26.5 ± 14.0/100 μm^2 (38 measurements in 17 cells, 38 electron micrographs). We expect that the immunolabeled foci at the fiber periphery include both peripheral couplings and peripherally located dyads, whereas clusters of particles detected in freeze-fracture correspond exclusively to peripheral couplings. Thus the density of foci is expected to be larger than the density of clusters. The measured ratio of fluorescent foci to particle cluster densities on the substrate side of the cell (1.46 from the above data) is slightly lower than the ratio of total peripheral junctions (periph-

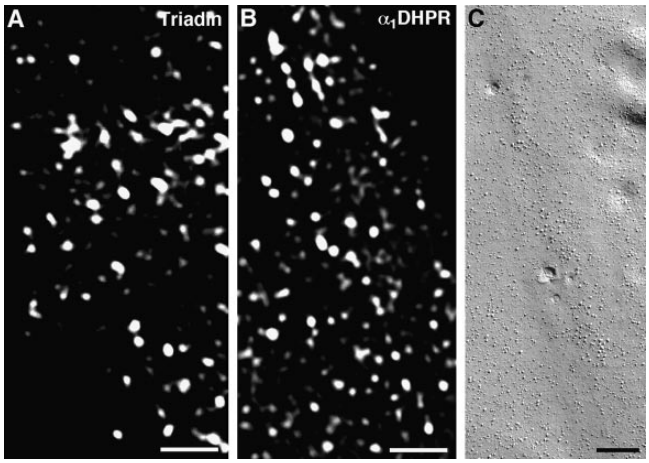

Figure 8. Triadin foci (*A*), DHPR foci (*B*), and clusters of large particles (*C*) are prominently aligned in a preferred orientation on the surface of some cells. The long axis of the cell is aligned along the diagonal of the images, as is the orientation of foci and particle cluster lines. Bars: (*A* and *B*) 5 μm; (*C*) 0.2 μm.

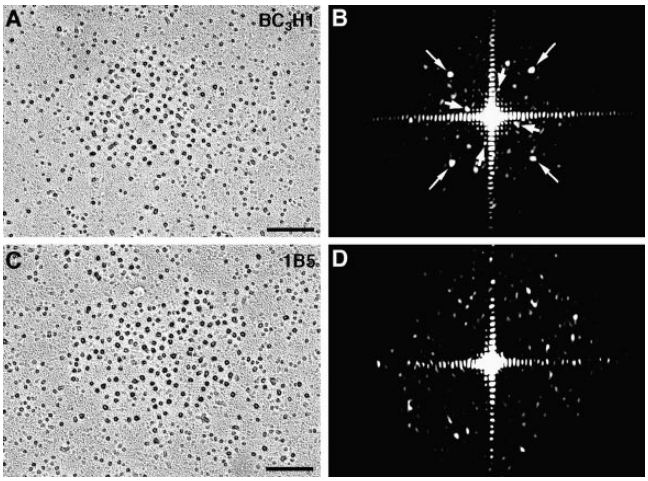

Figure 9. Rotary shadowing images of large particle clusters in BC_3H1 and 1B5 cells (*A* and *C*), and their respective optical diffraction patterns (*B* and *D*). The tetradic arrangement of DHPRs in BC_3H1 cells gives rise to a pattern (*B*) showing two orthogonal arrays rotated relative to each other that represent, respectively, the spacing between tetrads in the array (*small arrows*) and the spacing between particles within the tetrads (*large arrows*; see Protasi et al., 1997 for details). The disordered arrangement of particles in the clusters of 1B5 cells results in a diffraction pattern (*D*) without any special features. Bars, 0.1 μm.

eral couplings plus cortical dyads) to peripheral couplings (1.56 from counts in thin sections). The most probable cause for this minor discrepancy is that some of the fluorescent spots are likely to represent more than a single cluster of particles. Indeed, two or three peaks of density are often seen within some of the larger spots. Equal densities of DHPR foci and particle clusters suggests identity of the two structures. This is further supported by the following observations: (*a*) clusters of particles and foci of DHPR immunolabeling are present on many but not all differentiating cells; (*b*) clusters of particles and foci of DHPRs are randomly distributed in most cells; (*c*) in some cells, foci that immunostain positive for anti-DHPR antibodies are strikingly arranged in longitudinal rows (Figs. 7 *B*, and 8 *B*). A similar disposition is also observed for plasma membrane domains containing clusters of particles (Fig. 7 *D*, *arrows* and *semicircles*, and 8 *C*); and (*d*) some DHPR foci and particle clusters are so closely spaced that they almost fuse with each other (compare Fig. 8 *B* with *C*).

The above analysis suggests that the large, clustered particles in the surface of 1B5 cells are DHPRs. Indeed, the large particles in 1B5 clusters are identical in size with the particles representing DHPRs in the tetrads of BC_3H1 cells (Protasi et al., 1997), and are also quite similar to the slightly smaller particles representing DHPRs in cardiac muscle. The apparent diameter and height of the large, clustered particles in 1B5 cells is 9.9 and 10.9 nm, respectively (see above); the large particles forming tetrads in BC_3H1 cells are 9.7 ± 1.2-nm wide and 10.6 ± 1.8-nm tall (from 100 particles, 4 cells, 4 freeze-fractures); the particles in cardiac muscle are 8.5-nm wide and 9.6-nm tall (Sun et al., 1995).

Foci of triadin detected by immunolabeling are also located in prominent longitudinal rows (Figs. 7 *A*, and 8 *A*) and have density equal to DHPR foci (see above). Thus, the three detectable components of calcium release units of 1B5 cells (DHPR and triadin foci, detected by immunolabeling; and large particles, detected by freeze-fracture) appear to be colocalized. Since triadin is a junctional SR protein, this colocalization occurs at the junctions between SR and exterior membranes.

The Disposition of Skeletal DHPRs in 1B5 Cells Resembles That of Cardiac, Not Skeletal Muscle. Optical diffraction confirms the random disposition of DHPRs in 1B5 cells. Fig. 9 compares images from rotary shadowed replicas of *A* an array of tetrads in a peripheral coupling from the BC_3H1 cell line, and *C*, a group of DHPRs from a 1B5 cell. The optical transformation of the tetrad array (Fig. 9 *B*) shows evidence for two tetragonal arrangements indexing on the spacing between particles within the tetrad (Fig. 9 *B*, *large arrows*) and between the centers of tetrads (Fig. 9 *B*, *small arrows*; see Protasi et al., 1997). Note that tetrad arrays in BC_3H1 cells have identical parameters to those of other skeletal muscle both in vivo and in vitro (Franzini-Armstrong and Kish, 1995). The optical transformation of the 1B5 cluster (Fig. 9 *D*) shows only noise derived from the random arrangement of scattering units. This analysis confirms the visual impression that DHPRs in dyspedic junctions of 1B5 cells are randomly disposed and do not form tetradic arrays. The random disposition of DHPRs in peripheral junctional domains resembles that observed in cardiac muscle myocytes (Sun et al., 1995; Protasi et al., 1996; see Fig. 12 for a diagram).

Restoration of Tetrads After Transfection of 1B5 Cells with cDNA Encoding for the Ry_1R

Immunohistochemistry. 1B5 cells transfected with the cDNA for Ry_1R were immunolabeled with Ry_1R-specific antibody. 4–5 d after withdrawal of growth medium (D4–5)

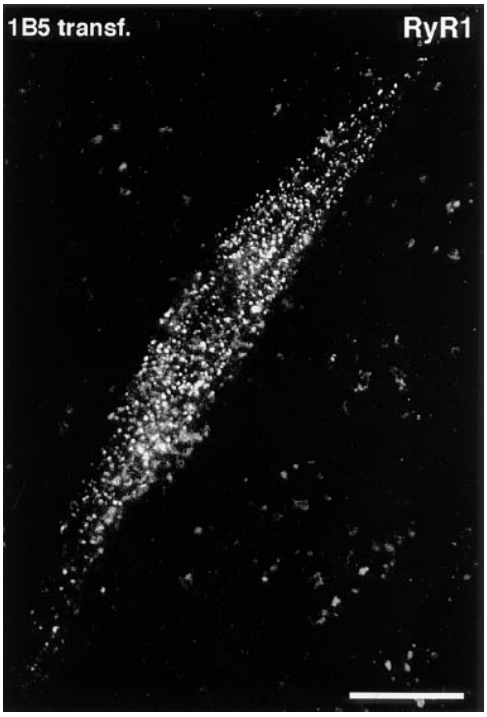

Figure 10. Immunolabeling with anti-Ry_1R antibodies in transfected 1B5 cells (4 d after differentiation). The plane of focus is close to the substrate side of the cell, which is flat. RyRs, similar to DHPRs and triadin, cluster in frequent, discrete foci at or near the cell surface (see Figs. 2, 3, 7, and 8). Bar, 25 μm.

~10% myotubes are positive for Ry_1R. These Ry_1R molecules are tightly clustered in discrete foci, similar to those found in normal developing skeletal muscle (Fig. 10; compare with Flucher et al., 1993*b*; Flucher et al., 1994). Similar to DHPR and triadin foci, Ry_1R immunopositive spots are mostly located on or near the surface membrane, on both ventral and dorsal sides of the myotubes. Nontransfected cells incubated with the same primary and secondary antibodies and transfected cells incubated with only the secondary antibody are negative.

Freeze Fracture. Freeze fracture of transfected cells shows restoration of tetrad arrays in the surface membrane of ~10% 1B5 cells. Fig. 11, *A–C* shows clusters of large particles (DHPRs) in the surface membrane of a dyspedic 1B5 cell (Fig. 11 *A*; see also Fig. 6), of a normal developing myotube (mouse) in vivo (Fig. 11 *B*), and of a transfected 1B5 cell (Fig. 11 *C*). In 1B5 cells, the particles have a random arrangement, whereas in normal myotubes and in transfected cells the particles are clearly arranged in tetrads (Fig. 11, *B* and *C*, *arrows*), and tetrads are part of an array. The forming arrays of tetrads in transfected 1B5 cells are always located on a slightly raised membrane mound, suggesting that they are located at sites where the SR is closely opposed to the surface membrane, forming a peripheral coupling. Tetrads, in the domains of both normal skeletal muscle and transfected 1B5 cells, are often incomplete, that is they miss one or more components (see also Takekura et al., 1994; Franzini-Armstrong and Kish, 1995; Protasi et al., 1997 for similar observations in a variety of muscle fibers and in the BC_3H1 cell line). Examples of

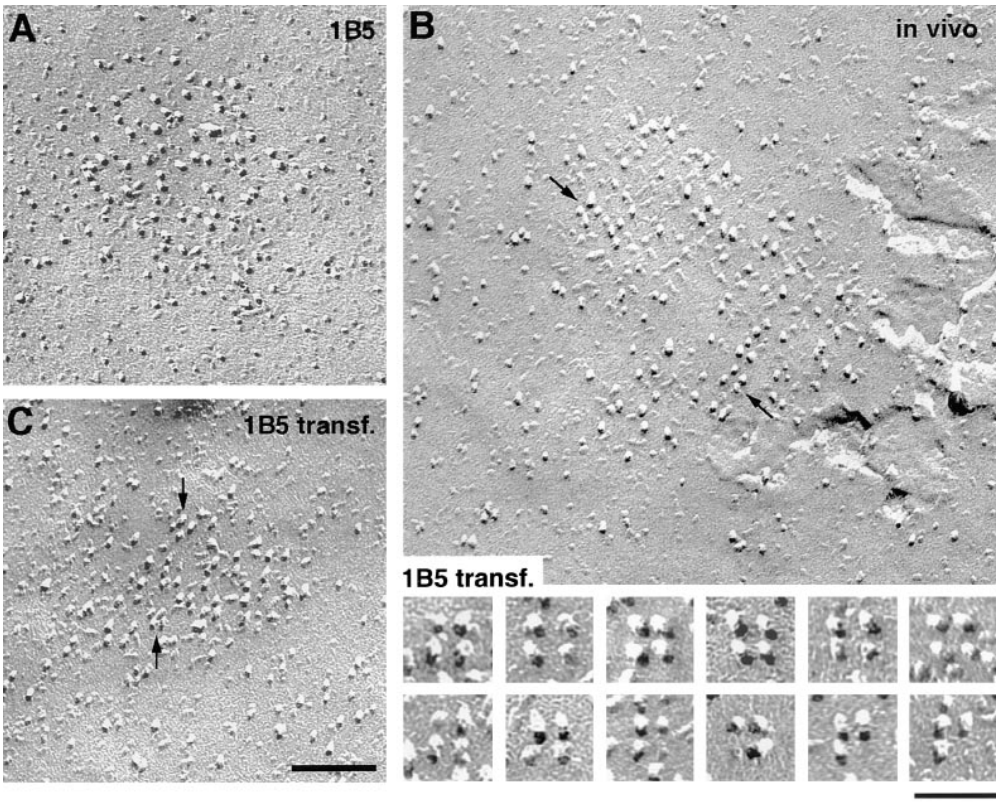

Figure 11. Restoration of tetrads in transfected 1B5 cells. (*A*) Domain of large particles in a dyspedic 1B5 cell; the particles, representing DHPRs, are randomly disposed (see also Figs. 6 and 9). (*B*) Array of tetrads in normal skeletal muscle (E18 mouse leg muscle); the large particles form tetrads (groups of four DHPRs; *arrows*), and tetrads are part of an ordered array. Several tetrads are incomplete (formed by only two or three elements). (*C*) Array of tetrads in a transfected 1B5 cell (4 d after differentiation); DHPRs are clearly arranged in tetrads (*arrows*), as in peripheral couplings of normal skeletal muscle. Details at the bottom of the figure show two sets of tetrads, complete (*top row*) and incomplete (*bottom row*). Note that: (*a*) complete tetrads can be slightly distorted; (*b*) the apparently missing components of incomplete tetrads may actually be elements (DHPRs) that broke during fracturing, leaving small stumps (see *bottom left*); and (*c*) some incomplete tetrads seem to lack one or more components (*bottom right*). Bars: (*A–C*) 0.1 μm; (*inset*) 0.05 μm.

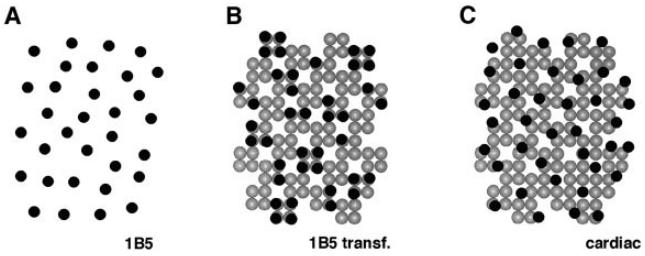

Figure 12. Diagrams showing the relation between RyRs and DHPRs in peripheral couplings of dyspedic 1B5 cells (*A*), transfected 1B5 cells (*B*), and cardiac muscle (*C*). RyRs (*gray*) form ordered arrays in the junctional SR of both skeletal and cardiac muscle. The array of feet are drawn as defined in Franzini-Armstrong and Kish (1995). Note that the array of feet in cardiac muscle is shown to be identical to that in skeletal muscle, although this is not known in detail. (*A*) Dyspedic 1B5 cells do not have feet; skeletal DHPRs (*black*) are not capable of forming tetrads on their own, in the absence of RyRs. (*B*) In Ry_1R-transfected 1B5 cells, as in normal skeletal muscle, DHPRs form tetrads that are located in exact correspondence of subunits of alternate feet, suggesting a link between the molecules. In *B*, tetrads have been drawn as they appear to be in fracture replicas; often incomplete but always associated with subunit of alternate feet. (*C*) In cardiac muscle, on the other hand, DHPRs do not form tetrads and their position relative to the feet subunits is variable, and thus a RyR–DHPR link is less likely.

complete tetrads and tetrads with one missing element from transfected 1B5 cells are shown at the bottom right of Fig. 11. Complete tetrads, formed by four large and tall particles disposed at the corners of a square, are shown in Fig. 11, *bottom right*, *top row*. A minor distortion of the precise square arrangement is sometimes introduced by the fracturing process. Incomplete tetrads with three components are shown in the bottom row. These are unequivocally identified as tetrads with one missing particle, because the three particles are of the same size, because they subtend a 90° angle, and because they are part of a "domain of large particles." Tetrads may be incomplete for different reasons: (*a*) one or more particle may break during fracturing and appear as a small stump (examples at left in the bottom row), or (*b*) components may be missing from the array, as shown in the last two examples at right in the bottom row (Protasi et al., 1997). Both situations are found in tetrads of normal myotubes developing in vivo and in vitro (see references above).

Discussion

During normal differentiation of cardiac and skeletal muscle, RyRs, DHPRs, and triadin are always coclustered within calcium release units, giving the impression that these proteins and their interactions play a major role in the formation of the junctions between the SR and exterior membranes (Yuan et al., 1991; Flucher et al., 1993*a*,*b*, 1994; Protasi et al., 1996; for reviews see Franzini-Armstrong and Jorgensen, 1994; Flucher and Franzini-Armstrong, 1996). However, observations of various model systems reveal that docking of the SR to exterior membranes may occur in the absence of either DHPRs or RyRs (Franzini-Armstrong et al., 1991; Flucher et al., 1993*b*; Takekura et al., 1995*b*; Takeshima et al., 1995; Powell et al., 1996; Takeshima et al., 1997). Junctions are also formed in the muscle fibers of Ry_1R/Ry_3R double knockout mice (Ikemoto et al., 1997), showing that the presence of a small amount of Ry_3R is not needed for SR/exterior membrane docking. In addition, in normal developing cardiac muscle, docking of the SR to the surface membrane precedes the localization of DHPRs and RyRs at the junctions (Protasi et al., 1996). Clustering of SR junctional proteins at calcium release units is also independent of the presence of DHPRs, since RyRs, triadin, and calsequestrin are present at SR–surface membrane junctions in dysgenic myotubes lacking α_1-DHPR (Franzini-Armstrong et al., 1991; Flucher et al., 1993*b*).

The findings in this study of dyspedic junctions add three further clues to the formation of calcium release units. The first is that DHPRs cluster at the junctions in the absence of RyRs. It must be assumed that other proteins of the junctional SR, perhaps even the same components that are responsible for SR–surface docking, have the role of holding DHPRs at the junctional sites. This is confirmed by the fact that CHO cells, which are of epithelial origin, seem to lack the component(s) needed for both docking of ER to the surface membranes and for extensive DHPR clustering, even when expression of skeletal RyR and a cardiac–skeletal DHPR chimera is induced in these cells (Takekura et al., 1995*a*).

A second result is that the presence of RyRs is not needed for the clustering of triadin in calcium release units. Two quite distinct roles have been proposed for triadin. On one hand, triadin is thought to reach out into the junctional gap between SR and surface membranes and either facilitate or directly participate in the joining of DHPRs to RyRs in skeletal muscle (Caswell et al., 1991; Fan et al., 1995*a*,*b*). On the other hand, the same molecule is described as being mostly located intraluminally, where it may help to link calsequestrin to the junctional SR membrane (Knudson et al., 1993*a*,*b*; Guo and Campbell, 1995). Our finding that triadin is present at the dyspedic junctions in the absence of RyRs does not help to solve the question of triadin function.

A third, and most important finding is that DHPRs do not associate into tetrads in the absence of Ry_1R (Figs. 11 *A*, and 12 *A*) and that tetrads are restored after "rescue" of the dyspedic phenotype by transfection of dyspedic cells with the Ry_1R cDNA (Figs. 11 *C*, and 12 *B*). These results provide direct confirmation of two current hypotheses on junctional architecture. One is that DHPRs are linked to RyRs in skeletal muscle and this linkage is responsible for the formation of tetrads (Block et al., 1988; Takekura et al., 1994; Protasi et al., 1997), and the other is that the random disposition of cardiac muscle DHPRs within junctional domains is, on the contrary, because of a lack of a link to the cardiac RyRs (Sun et al., 1995; see Fig. 12 *C*).

Present and past observations lead to the conclusion that the targeting of RyRs and DHPRs, as well as triadin and calsequestrin, to the junctional areas may be independent of each other and probably depend on other junctional components of a still unknown identity. However, one finding during the development of junctions in avian cardiac muscle seems at odds with this conclusion. Differ-

entiation of the calcium release units in this muscle involves an initial docking of the SR to the surface, and then a coordinated assembly of groups of feet and DHPRs, which do not fill the entire docked area, but cluster together on one side (Protasi et al., 1996).

A previous study of dyspedic skeletal muscle in vivo agrees with the results presented here in showing formation of junctions that lack feet, but differs because clusters of large particles (DHPRs) were not detected in the plasma membrane of dyspedic muscle in mouse (Takekura et al., 1995*b*). The reason for this difference is not clear, since mRNA for the DHPR is present in the in vivo dyspedic muscle (Takeshima et al., 1994), and the protein is expressed (although in reduced amounts; ~50% [Buck et al., 1997]). Also, charge movement is detected in primary cultures of dyspedic muscles (Nakai et al., 1996).

Muscle fibers of normal mouse express low but detectable levels of Ry_3R (Giannini et al., 1995). A few groupings of feet, presumably representing Ry_3R, have been detected in dyspedic myotubes developing in vivo (Takekura et al., 1995*b*), confirming functional evidence for caffeine-sensitive calcium release in primary dyspedic myotubes (Takeshima et al., 1995). In 1B5 cells, on the other hand, Ry_3R cannot be detected by biochemical approaches (Moore et al., 1998), and we have not found evidence for feet in thin sections from these cells suggesting that Ry_3R is not expressed in these cells at all.

1B5 and BC_3H1, two cell lines that express skeletal muscle–specific proteins of the junctional SR have three interesting structural defects in common: the cells either lack Z lines or have poorly developed ones; the nonjunctional sarcoplasmic reticulum is very poorly represented; peripheral couplings and junctions between SR and primitive T tubules on the other hand are relatively frequent. Since the nonjunctional SR develops early and is associated with the Z lines of myofibrils during normal skeletal muscle differentiation (Flucher et al., 1991, 1992, 1993*a*), the first two defects listed above may be causally linked.

The findings of this work highlight three important structural and developmental details of Ca^{2+} release units of muscle cells: the requirement of Ry_1R for the formation of tetrads, a structural feature of Ca^{2+} release units that is unique to skeletal muscle; the independence from RyRs of the association of triadin and DHPRs with the forming junctions; the independence from RyR of the initial docking of SR to exterior membranes. The restoration of tetrads in transfected 1B5 cells gives the ultimate demonstration that the DHPRs arrangement in tetrads is strictly dependent on their interaction, direct or not, with Ry_1R subunits.

We thank Drs. A.H. Caswell, K.P. Campbell, J.A. Airey, and J.L. Sutko for their generous gift of antibodies. We thank N. Glaser (University of Pennsylvania, Philadelphia, PA) for expert assistance and R. Moore (University of California, Davis, CA) for helpful suggestions on transfection procedures.

This work was supported by National Institutes of Health grants R01 HL48093 to the Pennsylvania Muscle Institute (to C. Franzini-Armstrong), and R01AR43140 (to P.D. Allen), and by a grant from The Muscular Dystrophy Association (to P.D. Allen).

Received for publication 5 May 1997 and in revised form 21 November 1997.

References

Adams, B.A., T. Tanabe, A. Mikami, S. Numa, and K.G. Beam. 1990. Intramembrane charge movement restored in dysgenic skeletal muscle by injection of dihydropyridine receptor cDNAs. *Nature.* 346:569–572.

Airey, J.A., C.F. Beck, K. Murakami, S.J. Tanksley, T.J. Deerinck, M. Ellsiman, and J.L. Sutko. 1990. Identification and localization of two triad junction foot protein isoforms in mature avian fast twitch skeletal muscle. *J. Biol. Chem.* 265:14187–14194.

Ashely, C.C., I.P. Mulligan, and T.J. Lea. 1991. Ca^{2+} and activation mechanisms in skeletal muscle. *Rev. Biophys.* 24:1–73.

Block, B.A., T. Imagawa, K.P. Campbell, and C. Franzini-Armstrong. 1988. Structural evidence for direct interaction between the molecular components of the transverse tubule/sarcoplasmic reticulum junction in skeletal muscle. *J. Cell Biol.* 107:2587–2600.

Brandt, N.R., A.H. Caswell, S.-N. Wen, and J.A. Talvenheimo. 1990. Molecular interactions of the junctional foot protein and dihydropyridine receptor in skeletal muscle triads. *J. Membr. Biol.* 113:237–251.

Buck, E.D., A.H. Nguyen, I.N. Pessah, and P.D. Allen. 1997. Dyspedic mouse skeletal muscle expresses major elements of the triadic junction but lacks ryanodine receptor protein and function. *J. Biol. Chem.* 272:7360–7367.

Campbell, K.P., C.M. Knudson, T. Imagawa, A.T. Leung, J.L. Sutko, S.D. Kahl, C. Reynolds-Raab, and L. Madson. 1987. Identification and characterization of the high affinity [^{3}H]ryanodine receptor of the junctional sarcoplasmic reticulum Ca^{2+} release channel. *J. Biol. Chem.* 262:6460–6463.

Carl, S.L, K. Felix, A.H. Caswell, N.R. Brandt, W.J. Ball, P.L. Vaghy, G. Meissner, and D.G. Ferguson. 1995*a.* Immunolocalization of sarcolemmal dihydropyridine receptor and sarcoplasmic reticular triadin and ryanodine receptor in rabbit ventricle and atrium. *J. Cell Biol.* 129:672–682.

Carl, S.L, K. Felix, A.H. Caswell, N.R. Brandt, J.P. Brunschwig, G. Meissner, and D.G. Ferguson. 1995*b.* Immunolocalization of triadin, DHP receptors, and ryanodine receptors in adult and developing skeletal muscle of rats. *Muscle Nerve.* 18:1232–1243.

Caswell, A.H., N.R. Brandt, J.P. Brunschwig, and S. Purkerson. 1991. Localization and partial characterization of the oligomeric disulfide-linked molecular weight 95,000 protein (triadin) which binds the ryanodine and dihydropyridine receptors in skeletal muscle triadic vesicles. *Biochemistry.* 30:7507–7513.

Cohen, S.A., and D.W. Pumplin. 1979. Clusters of intramembranous particles associated with binding sites for alpha-bungarotoxin in cultured chick myotubes. *J. Cell Biol.* 82:494–516.

Coronado, R., J. Morrissette, M. Sukhareva, and D.M. Vaughan. 1994. Structure and function of ryanodine receptors. *Am. J. Physiol.* 266:1485–1491.

Fabiato, A. 1983. Calcium-induced release of calcium from cardiac sarcoplasmic reticulum. *Am. J. Physiol.* 245:1–14.

Fan, H., N.R. Brandt, M. Peng, A. Schwartz, and A.H. Caswell. 1995*a.* Binding sites of monoclonal antibodies and dihydropyridine receptor α_1 subunit cytoplasmic II-III loop on skeletal muscle triadin fusion peptides. *Biochemistry.* 34:14893–14901.

Fan, H., N.R. Brandt, and A.H. Caswell. 1995*b.* Disulfide bonds, N-glycosylation and transmembrane topology of skeletal muscle triadin. *Biochemistry.* 34:14902–14908.

Flucher, B.E., and C. Franzini-Armstrong. 1996. Formation of junctions involved in excitation-contraction coupling in skeletal and cardiac muscle. *Proc. Natl. Acad. Sci. USA.* 93:8101–8106.

Flucher, B.E., M.E. Morton, S.C. Froehner, and M.P. Daniels. 1990. Localization of the α_1 and α_2 subunits of the dihydropyridine receptor and ankyrin in skeletal muscle triads. *Neuron.* 5:339–351.

Flucher, B.E., M. Terasaki, H. Chin, T. Beeler, and M.P. Daniels. 1991. Biogenesis of transverse tubules in skeletal muscle in vitro. *Dev. Biol.* 145:77–90.

Flucher, B.E., J.L. Phillips, J.A. Powell, S.B. Andrews, and M.P. Daniels. 1992. Coordinated development of myofibrils, sarcoplasmic reticulum and transverse tubules in normal and dysgenic mouse skeletal muscle, *in vivo* and *in vitro. Dev. Biol.* 150:266–280.

Flucher, B.E., H. Takekura, and C. Franzini-Armstrong. 1993*a.* Development of the excitation-contraction coupling apparatus in skeletal muscle: association of sarcoplasmic reticulum and transverse tubules with myofibrils. *Dev. Biol.* 160:135–147.

Flucher, B.E., S.B. Andrews, S. Fleisher, A.R. Marks, A.H. Caswell, and J.A. Powell. 1993*b.* Triad formation: Organization and function of the sarcoplasmic reticulum calcium release channel and triadin in normal and dysgenic muscle in vitro. *J. Cell Biol.* 123:1161–1174.

Flucher, B.E., S.B. Andrews, and M.P. Daniels. 1994. Molecular organization of transverse tubule/sarcoplasmic reticulum junctions during development of excitation-contraction coupling in skeletal muscle. *Mol. Biol. Cell.* 5:1105–1118.

Fosset, M., E. Jaimovich, E. Delpont, and M. Lazdunski. 1983. [^{3}H]nitrendipine receptors in skeletal muscle. *J. Biol. Chem.* 258:6086–6092.

Franzini-Armstrong, C. 1970. Studies of the triad. *J. Cell Biol.* 47:488–499.

Franzini-Armstrong, C. 1991. Simultaneous maturation of transverse tubules and sarcoplasmic reticulum during muscle differentiation in the mouse. *Dev. Biol.* 146:353–363.

Franzini-Armstrong, C., and G. Nunzi. 1983. Junctional feet and particles in the triads of fast-twitch muscle fibers. *J. Muscle Res. Cell Motil.* 4:233–252.

Franzini-Armstrong, C., and A.O. Jorgensen. 1994. Structure and development

of e-c coupling units in skeletal muscle. *Annu. Rev. Physiol.* 56:509–534.
Franzini-Armstrong, C., and J.W. Kish. 1995. Alternate disposition of tetrads in peripheral couplings of skeletal muscle. *J. Muscle Res. Cell Motil.* 16:319–324.
Franzini-Armstrong, C., and F. Protasi. 1997. The ryanodine receptor of striated muscles, a complex capable of multiple interactions. *Physiol. Rev.* 77: 699–729.
Franzini-Armstrong, C., M. Pincon-Raymond, and F. Rieger. 1991. Muscle fibers from dysgenic mouse *in vivo* lack a surface component of peripheral couplings. *Dev. Biol.* 146:364–376.
Giannini, G., A. Conti, S. Mammarella, M. Scrobogna, and V. Sorrentino. 1995. The ryanodine receptor/calcium channel genes are widely and differentially expressed in murine brain and peripheral tissues. *J. Cell Biol.* 128:893–904.
Guo, W., and K.P. Campbell. 1995. Association of triadin with the ryanodine receptor and calsequestrin in the lumen of sarcoplasmic reticulum. *J. Biol. Chem.* 270:9027–9030.
Guo, W., A.O. Jorgensen, K.P. Campbell. 1994. Characterization and ultrastructural characterization of a novel 90kDa protein unique to skeletal muscle junctional sarcoplasmic reticulum. *J. Biol. Chem.* 269:28359–28365.
Guo, W., A.O. Jorgensen, L.R. Jones, and K.P. Campbell. 1996. Biochemical characterization and molecular cloning of cardiac triadin. *J. Biol. Chem.* 271: 458–465.
Ikemoto, T., S. Komazaki, H. Takeshima, M. Nishi, T. Noda, M. Iino, and M. Endo. 1997. Functional and morphological features of skeletal muscle from mutant mice lacking both type 1 and type 3 ryanodine receptors. *J. Physiol. (Lond).* 501:305–312.
Imagawa, T., J.S. Smith, R. Coronado, and K.P. Campbell. 1987. Purified ryanodine receptor from skeletal muscle sarcoplasmic reticulum is the Ca^{2+} permeable pore of the calcium release channel. *J. Biol. Chem.* 262:16636–16643.
Inui, M., A. Saito, and S. Fleischer. 1987. Purification of the ryanodine receptor and identity with feet structures of junctional terminal cisternae of sarcoplasmic reticulum from fast skeletal muscle. *J. Biol. Chem.* 262:1740–1747.
Ishikawa, H. 1968. Formation of elaborate networks of T-systems tubules in cultured skeletal muscle with special reference to the T-system formation. *J. Cell Biol.* 38:51–66.
Jorgensen, A.O., A.C-Y. Shen, W. Arnold, A.T. Leung, and K.P. Campbell. 1989. Subcellular distribution of the 1,4-dihydropyridine receptor in rabbit skeletal muscle in situ: an immunofluorescence and immunocolloidal gold-labeling study. *J. Cell Biol.* 109:135–147.
Kawamoto, R.M., J.P. Brunschwig, K.C. Kim, and A.H. Caswell. 1986. Isolation, characterization, and localization of the spanning protein from skeletal muscle triads. *J. Cell. Biol.* 103:1405–1414.
Kim, K.C., A.H. Caswell, J.A. Talvenheimo, and N.R. Brandt. 1990. Isolation of a terminal cisterna protein which may link the dihydropyridine receptor to the junctional foot protein in skeletal muscle. *Biochemistry.* 29:9281–9289.
Knudson, C.M., N. Chaudari, A.H. Sharp, J.A. Powell, K.G. Beam, and K.P. Campbell. 1989. Specific absence of the α_1 subunit of the dihydropyridine receptor in mice with muscular dysgenesis. *J. Biol. Chem.* 264:1345–1348.
Knudson, C.M., K.K. Stang, A.O. Jorgensen, and K.P. Campbell. 1993*a.* Biochemical characterization and ultrastructural localization of a major junctional sarcoplasmic reticulum glycoprotein (triadin). *J. Biol. Chem.* 268: 12637–12645.
Knudson, C.M., K.K. Stang, C.R. Moomaw, C.A. Slaughter, and K.P. Campbell. 1993*b.* Primary structure and topological analysis of a skeletal muscle-specific junctional sarcoplasmic reticulum glycoprotein (triadin). *J. Biol. Chem.* 268:12646–12654.
Lai, F.A., H.P. Erickson, E. Rousseau, Q.Y. Liu, and G. Meissner. 1988. Purification and reconstitution of the calcium release channel from skeletal muscle. *Nature.* 331:315–319.
Leung, A.T., T. Imagawa, and K.P. Campbell. 1987. Structural characterization of the 1,4-dihydropyridine receptor of the voltage-dependent Ca^{2+} channel from rabbit skeletal muscle. Evidence for two distinct high molecular weight subunits. *J. Biol. Chem.* 262:7943–7946.
Meissner, G. 1975. Isolation and characterization of two types of sarcoplasmic reticulum vesicles. *Biochim. Biophys. Acta.* 389:51–68.
Meissner, G. 1994. Ryanodine receptor/Ca^{2+} release channels and their regulation by endogenous effectors. *Annu. Rev. Physiol.* 56:485–508.
Moore, R.A., H. Nguyen, J. Galceran, I.N. Pessah, and P.D. Allen. 1998. A transgenic myogenic cell line lacking ryanodine receptor protein for homologous expression studies: Reconstitution of Ry_1R protein and function. *J. Cell Biol.* 140:843–851.
Mortensen, R.M., D.A. Conner, S. Chao, A.A. Geisterfer-Lowrance, and J.G. Seidman. 1992. Production of homozygous mutant ES cells with a single targeting construct. *Mol. Cell. Biol.* 12:2391–2395.
Morton, M.E., and S.C. Froehner. 1987. Monoclonal antibody identifies a 200-kDa subunit of the dihydropyridine-sensitive calcium channel. *J. Biol. Chem.* 262:11904–11907.
Morton, M.E., and S.C. Froehner. 1989. The α_1 and α_2 polypeptides of the dihydropyridine-sensitive calcium channel differ in developmental expression and tissue distribution. *Neuron.* 2:1499–1506.
Nakai, J., R.T. Dirksen, H.T. Nguyen, I.N. Pessah, K.G. Beam, and P.D. Allen. 1996. Enhanced dihydropyridine receptor channel activity in the presence of ryanodine receptor. *Nature.* 380:72–75.
Nakai, J., T. Ogura, F. Protasi, C. Franzini-Armstrong, P.D. Allen, and K.G. Beam. 1997. Functional non equality of the cardiac and skeletal ryanodine receptors. *Proc. Natl. Acad. Sci. USA.* 94:1019–1022.
Osame, M., A.G. Engel, C.J. Rebouche, and R.E. Scott. 1981. Freeze-fracture electron microscopic analysis of plasma membranes of cultured muscle cells in Duchenne dystrophy. *Neurology.* 31:972–979.
Pincon-Raymond, M., F. Rieger, M. Fosset, and M. Lazdunski. 1985. Abnormal transverse tubule system and abnormal amount of receptors for Ca^{2+} channel inhibitors of the dihydropyridine family in skeletal muscle from mice with embryonic muscular dysgenesis. *Nature.* 325:717–720.
Powell, J.A., L. Petherbridge, and B.E. Flucher. 1996. Formation of triads without the dihydropyridine receptor α_1 subunits in cell lines from dysgenic skeletal muscle. *J. Cell Biol.* 134:375–387.
Protasi, F., X-H. Sun, and C. Franzini-Armstrong. 1996. Formation and maturation of calcium release apparatus in developing and adult avian myocardium. *Dev. Biol.* 173:265–278.
Protasi, F., C. Franzini-Armstrong, and B.E. Flucher. 1997. Coordinated incorporation of skeletal muscle dihydropyridine receptors and ryanodine receptors in peripheral couplings of BC_3H1 cells. *J. Cell Biol.* 137:859–870.
Radermacher, M., V. Rao, R. Grassucci, J. Frank, A.P. Timerman, S. Fleisher, and T. Wagenknecht. 1994. Cryo-electron microscopy and three-dimensional reconstruction of the calcium release channel/ryanodine receptor from skeletal muscle. *J. Cell Biol.* 127:411–423.
Pozzan, T., R. Rizzuto, P. Volpe, and J. Meldolesi. 1994. Molecular and cellular physiology of intracellular calcium stores. *Physiol. Revs.* 74:595–636.
Rios, E., and G. Brum. 1987. Involvement of dihydropyridine receptors in excitation-contraction coupling in skeletal muscle. *Nature.* 325:717–720.
Rios, E., J. Ma, and A. Gonzales. 1991. The mechanical hypothesis of excitation contraction coupling. *J. Muscle Res. Cell Motil.* 12:127–135.
Santana, L.F., H. Cheng, A.M. Gomez, M.B. Cannell, and W.J. Lederer. 1996. Relation between the sarcolemmal Ca^{2+} current and Ca^{2+} sparks and local control theories for cardiac excitation-contraction coupling. *Circ. Res.* 78: 166–171.
Sham, J.S., L. Cleemann, and M. Morad. 1995. Functional coupling of Ca^{2+} channels and ryanodine receptors in cardiac myocytes. *Proc. Natl. Acad. Sci. USA.* 92:121–125.
Schneider, M.F. 1981. Membrane charge movements and depolarization-contraction coupling. *Annu. Rev. Physiol.* 43:507–517.
Schneider, M.F., and W.K. Chandler. 1973. Voltage dependence charge movement in skeletal muscle: a possible step in excitation contraction coupling. *Nature.* 242:244–246.
Sun, X-H., F. Protasi, M. Takahashi, H. Takeshima, D.G. Ferguson, and C. Franzini-Armstrong. 1995. Molecular architecture of membranes involved in excitation-contraction coupling of cardiac muscle. *J. Cell Biol.* 129:659–671.
Sutko, J.L., and J.A. Airey. 1997. Ryanodine receptor Ca^{2+} release channel: does diversity in form equal diversity in function? *Physiol. Rev.* 76:1027–1071.
Takekura, H., L. Bennet, T. Tanabe, K.G. Beam, and C. Franzini-Armstrong. 1994. Restoration of junctional tetrads in dysgenic myotubes by dihydropyridine receptor cDNA. *Biophys. J.* 67:793–804.
Takekura, H., H. Takeshima, S. Nishimura, M. Takahashi, T. Tanabe, V. Flockerzi, F. Hoffman, and C. Franzini-Armstrong. 1995*a.* Co-expression in CHO cells of two muscle proteins involved in e-c coupling. *J. Muscle Res. Cell Motil.* 16:465–480.
Takekura, H., M. Nishi, T. Noda, H. Takeshima, and C. Franzini-Armstrong. 1995*b.* Abnormal junctions between surface membrane and sarcoplasmic reticulum in skeletal muscle with a mutation targeted to the ryanodine receptor. *Proc. Natl. Acad. Sci. USA.* 92:3381–3385.
Takeshima, H., M. Iino, H. Takekura, M. Nishi, J. Kuno, O. Minowa, H. Takano, and T. Noda. 1994. Excitation-contraction uncoupling and muscular degeneration in mice lacking functional skeletal muscle ryanodine-receptor gene. *Nature.* 369:556–559.
Takeshima, H., T. Yamazawa, T. Ikemoto, H. Takekura, M. Nishi, T. Noda, and M. Iino. 1995. Ca^{2+}-induced Ca^{2+} release in myocytes from dyspedic mice lacking the type-1 ryanodine receptor. *EMBO (Eur. Mol. Biol. Organ.) J.* 14:2999–3006.
Tanabe, T., H. Takeshima, A. Mikami, V. Flockerzi, H. Takahashi, K. Kangawa, M. Kojioma, H. Matsuo, T. Hirose, and S. Numa. 1987. Primary structure of the receptor for calcium channel blockers from skeletal muscle. *Nature.* 328:313–318.
Tanabe, T., K.G. Beam, J.A. Powell, and S. Numa. 1988. Restoration of excitation-contraction coupling and slow calcium current in dysgenic muscle by dihydropyridine receptor complementary DNA. *Nature.* 336:134–139.
Yuan, S., W. Arnold, and A.O. Jorgensen. 1991. Biogenesis of transverse tubules and triads: Immunolocalization of the 1,4-dihydropyridine receptor, TS28, and the ryanodine receptor in rabbit skeletal muscle developing in situ. *J. Cell Biol.* 112:289–301.